Langmuir

Article

pubs.acs.org/Langmuir

Photoreversible Micellar Solution as a Smart Drag-Reducing Fluid for Use in District Heating/Cooling Systems

Haifeng Shi,[†] Wu Ge,[†,§] Hyuntaek Oh,[⊥] Sean M. Pattison,[†] Jacob T. Huggins,[†] Yeshayahu Talmon,[∥] David J. Hart,[‡] Srinivasa R. Raghavan,[⊥] and Jacques L. Zakin*[,†]

[†]Department of Chemical and Biomolecular Engineering and [‡]Department of Chemistry and Biochemistry, Ohio State University, 100 West 18th Avenue, Columbus, Ohio 43210, United States

[§]Analytical Sciences, Mondelēz International, 200 Deforest Avenue, East Hanover, New Jersey 07936, United States

[∥]Department of Chemical Engineering, Technion-Israel Institute of Technology, Haifa 32000, Israel

[⊥]Department of Chemical and Biomolecular Engineering, University of Maryland, College Park, Maryland 20742-2111, United States

ABSTRACT: A photoresponsive micellar solution is developed as a promising working fluid for district heating/cooling systems (DHCs). It can be reversibly switched between a drag reduction (DR) mode and an efficient heat transfer (EHT) mode by light irradiation. The DR mode is advantageous during fluid transport, and the EHT mode is favored when the fluid passes through heat exchangers. This smart fluid is an aqueous solution of cationic surfactant oleyl bis(2-hydroxyethyl)methyl ammonium chloride (OHAC, 3.4 mM) and the sodium salt of 4-phenylazo benzoic acid (ACA, 2 mM). Initially, ACA is in a trans configuration and the OHAC/ACA solution is viscoelastic and exhibits DR (of up to 80% relative to pure water). At the same time, this solution is not effective for heat transfer. Upon UV irradiation, *trans*-ACA is converted to *cis*-ACA, and in turn, the solution is converted to its EHT mode (i.e., it loses its viscoelasticity and DR) but it now has a heat-transfer capability comparable to that of water. Subsequent irradiation with visible light reverts the fluid to its viscoelastic DR mode. The above property changes are connected to photoinduced changes in the nanostructure of the fluid. In the DR mode, the OHAC/*trans*-ACA molecules assemble into long threadlike micelles that impart viscoelasticity and DR capability to the fluid. Conversely, in the EHT mode the mixture of OHAC and *cis*-ACA forms much shorter cylindrical micelles that contribute to negligible viscoelasticity and effective heat transfer. These nanostructural changes are confirmed by cryo-transmission electron microscopy (cryo-TEM), and the photoisomerization of *trans*-ACA and *cis*-ACA is verified by ^{1}H NMR.

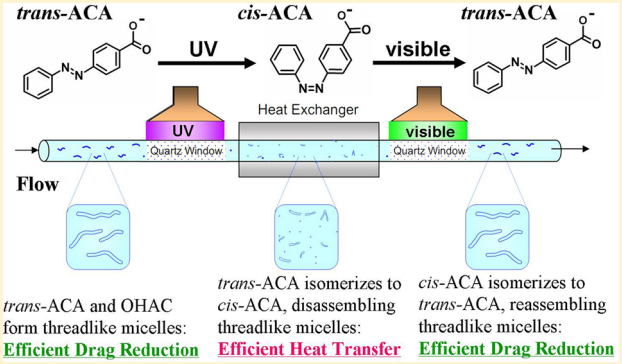

1. INTRODUCTION

Some cationic surfactants in the presence of organic counterions self-assemble into threadlike micelles (TLMs) in aqueous solutions.[1,2] These TLMs, resembling polymer molecules, entangle with each other and thereby impart non-Newtonian behavior to the fluid, such as viscoelasticity,[3,4] flow birefringence,[5,6] and shear-induced structure.[5,7,8] One striking characteristic of TLM solutions is their drag reduction (DR) behavior, which means that these fluids have significantly lower pressure loss in turbulent flow compared to water.[9] The %DR, defined as the reduction in drag in the presence of TLMs relative to pure water, can reach 80% or more.[10−12] This remarkable reduction in pressure loss translates to lower energy requirements for pumping fluids in recirculating systems.

A promising application of DR fluids is in district heating/cooling systems (DHCs)[9,11−15] in which hot or chilled water is recirculated. DHCs provide heated or chilled water from a central station to buildings in a district for heating or for air conditioning. With centralized equipment, such systems can achieve efficiencies by eliminating furnaces, boilers, and air conditioners in each building in a district. DHCs can utilize many kinds of energy sources from coal to geothermal, from natural gas to biomass. This flexibility makes DHCs more competitive in a time of increasingly expensive fuels.[9,16] Currently, DHCs are widely used in Europe, Japan, and Korea and are attracting increased interest in the United States.[16] The energy consumption for pumping water usually takes up about 15% of the entire energy cost of a DHC.[17] The pumping energy consumption can be reduced by using a drag-reducing water solution as a substitute for water. However, drag-reducing fluids have a reduced heat-transfer capability compared to that of water, and the %HTR (reduction in heat transfer relative to water) is usually a little higher than the %DR.[18−20] Therefore, it is of practical importance to enhance the heat-transfer capability of the drag-reducing solution in the

Received: October 8, 2012
Revised: December 3, 2012
Published: December 4, 2012

   dx.doi.org/10.1021/la304001r | *Langmuir* 2013, 29, 102−109

heat exchangers while maintaining the DR capability in the rest of the DHCs.

One advantage of surfactant-based (i.e., TLM-containing) DR solutions is that they regain their DR effectiveness after mechanical degradation when passing through pumps, whereas polymer-based DR solutions become permanently degraded by the shearing action of the pump.[21,22] In TLM-based drag-reducing flows, suppressed velocity fluctuations in the radial direction[23,24] and a reduced frequency of turbulent bursts[25,26] have been observed. These reduced turbulent characteristics are caused by the interaction between TLMs and the solvent. Long TLMs damp turbulent eddies,[27] and their alignment along the flow suppresses fluid movement in the direction normal to the flow.[23] The reduced turbulence results in reduced heat transfer in the radial direction. To enhance the heat transfer at the heat exchanger, the TLMs must be destroyed or the turbulence must be intensified. Mechanical methods to disrupt the TLMs include in-flow mechanical devices such as helical pipes,[10] fluted-tube heat exchangers,[28] wire meshes,[29] static mixers at the heat exchanger entrance,[30] and vortex generators.[12,31] However, all of these methods directly interfere with fluid flow, resulting in significant pressure losses. Alternatively, external stimuli have been studied to intensify turbulence in the heat exchanger. Qi et al.[32] used ultrasonic energy to externally enhance heat transfer, but this method was only partially effective and required a large energy cost.

In a recent study, we proposed the use of light irradiation as an external stimulus to switch between modes of drag reduction (DR) and enhanced heat transfer (EHT) in TLM-based fluids.[33] The concept for the application of this photoswitchable fluid is shown in Scheme 1. At the entrance to the heat exchanger, the fluid is irradiated by a light source to alter the molecular configuration of the surfactant/counterion in such a way that the TLMs are transformed into much shorter structures. The resulting fluid becomes nonviscoelastic and hence non-drag-reducing. At the same time, its waterlike behavior ensures an enhanced heat-transfer (EHT) capability. At the exit of the heat exchanger, a different light source is used to restore the original configuration of the surfactant/counterion, thus regenerating TLMs and giving the fluid its DR capability. This concept is based on the fact that the molecular geometry of the surfactant and counterion dictates the formation of TLMs or other micellar structures.[34−36]

Scheme 1. Use of Reversible Photoresponsive Fluids to Enhance Heat Transfer in a Heat Exchanger Temporarily

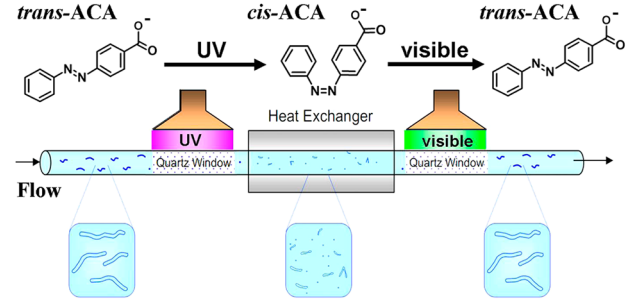

Although many photoresponsive surfactant systems have been reported in the literature,[37−41] few are based on low-cost or commercially available components. In our previous study,[33] we used a low-cost photoresponsive system originally developed by Ketner et al.[40] made of a long-tailed cationic surfactant with the organic counterion *trans-ortho*-methoxycinnamic acid (*trans*-OMCA). The attractive feature of this system is that *trans*-OMCA is inexpensive and commercially available. The surfactant and *trans*-OMCA solution had TLMs (and thus DR properties). Upon UV irradiation, *trans*-OMCA was irreversibly isomerized to *cis*-OMCA, causing the fluid to lose its TLMs and hence its viscoelasticity. Thereby, the fluid could be switched from a DR mode to an EHT mode. The DR could not be regained, however, because the counterion could not be photoisomerized in the reverse direction.

In the present work, we have improved our earlier design by using a reversibly photoswitchable organic counterion, viz., 4-phenylazo benzoic acid (ACA). Azobenzene derivatives are well known to undergo reversible photoisomerization.[42−50] We draw on recent work by Raghavan and co-workers,[51,52] who have reported a series of fluids based on ACA that exhibit dramatic, reversible changes in fluid viscosity. In that study, the surfactant used was erucyl bis(2-hydroxyethyl)methyl ammonium chloride (EHAC), a cationic surfactant with an unsaturated C_{22} tail. Here we employ a related cationic surfactant, oleyl bis(2-hydroxyethyl)methyl ammonium chloride (OHAC), which has an unsaturated C_{18} tail. Both EHAC and OHAC are commercially available at low cost, and ACA is also commercially available, although somewhat expensive. However, ACA is relatively easy to synthesize, and we have done so for this study. In turn, we have been able to prepare OHAC/ACA fluids in the large quantities (6 L) required for laboratory experiments in a recirculation loop.

We select OHAC over EHAC as the cationic surfactant for two reasons. First, the EHAC/ACA system requires a relatively high concentration (40 mM/20 mM, typically) in order to show significant changes in rheological properties induced by light irradiation. But for large-scale applications such as DHCs, it is of practical importance to have the additive concentration as low as possible. Second, our preliminary experiments showed that the UV-irradiated EHAC/ACA solution lost its viscoelasticity, and thus its drag reduction, only a few minutes after its was pumped in our recirculation system. This is probably due to the EHAC molecule's bulkier structure, which requires a longer time to reassemble with ACA than OHAC. We show that the OHAC/ACA solution, at the low concentration of 3.4 mM/2 mM, is drag-reducing with ACA in the trans configuration and can be switched between DR and EHT modes using UV and visible light, respectively, as indicated in Scheme 1. Thus, this fluid is ideal for recirculating DHCs because it saves pumping energy during flow and provides good heat transfer at the heat exchangers.

2. EXPERIMENTAL SECTION

2.1. Materials and Sample Preparation. The surfactant used in this study was donated by Akzo Nobel; its commercial name is Ethoquad O/12 PG. The commercial product contains alkyl bis(2-hydroxyethyl)methyl ammonium chlorides (82 wt %) with propylene glycol (18 wt %) as the solvent. The alkyl groups consist of about 82% oleyl (i.e., unsaturated C_{18}), 12% saturated C_{16}, 4% saturated C_{14}, and 1% saturated C_{12}. We denote the surfactant by the major component, viz., oleyl bis(2-hydroxyethyl)methyl ammonium chloride (OHAC, Scheme 2). The counterion, ACA (purity >99%), was synthesized from *p*-aminobenzoic acid (99%, Alfa Aesar) and nitrosobenzene

dx.doi.org/10.1021/la304001r | *Langmuir* 2013, 29, 102−109

Scheme 2. Molecular Structure of Cationic Surfactant OHAC

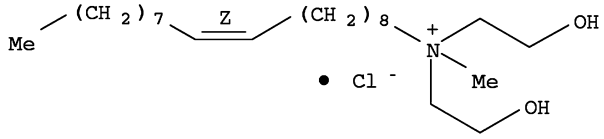

(97%, Sigma-Aldrich) and purified by recrystallization.[53] In the initial state, ACA is mostly in the *trans* configuration.

The OHAC/ACA solutions in small quantities were prepared by mixing the two compounds in water using magnetic stirrers. Samples were stirred overnight before rheological and other analytical measurements were made. Large quantities of solutions for drag reduction and heat-transfer experiments were prepared by stirring the solution in a bucket for 8 h at room temperature with a high-shear disperser (Janke & Hunkel IKA Ultra-Turrax SD-45). The solution pH was neutralized using sodium hydroxide. All of the solutions were well covered during preparation and storage to minimize exposure to light.

2.2. Light Irradiation. A 100 W Black-Ray long-wave UV lamp (broad band centered at 365 nm) and a 15 W LED lamp (radiation peaked at 450 nm) were used to irradiate samples. For UV−vis, rheology, cryo-TEM, and ^{1}H NMR measurements, 10 mL of a sample solution was placed in a Petri dish and irradiated for 30 min. For DR and heat-transfer experiments, 6 L of solution was divided into 12 batches of 500 mL. Each batch was held in a crystallizing dish and was irradiated with stirring for 3 h. To minimize isomerization after irradiation, each batch was covered and placed in a −20 °C freezer as soon as irradiation was completed. The day after irradiation and freezing, DR and heat-transfer measurements were made on irradiated samples.

2.3. Rheological Measurements. Shear viscosity (η) and the first normal stress difference (N_1) were measured with an ARES rheometer (TA Instruments) with a 50 mm cone-and-plate tool (0.02 rad cone angle and 0.056 mm gap) over a range of shear rates. Measured N_1 readings were corrected for inertial effects according to the following relation[54]

$$N_1^{\text{corrected}} = N_1^{\text{measured}} + 0.15\rho\omega^2R^2 \quad (1)$$

where ρ is the density of the solution, ω is the angular velocity, and R is the radius of the cone.

2.4. UV−Vis Spectroscopy and Cryo-TEM. Sample solutions for UV−vis spectra were first irradiated and then diluted 100-fold. UV−vis spectra were collected at room temperature on a Genesys 6 UV−vis spectrophotometer (Thermo Electron Corporation). Samples for cryo-TEM imaging were prepared and frozen at Ohio State University and shipped, with dry ice, to the Technion Laboratory for Electron Microscopy of Soft Matter, where cryo-TEM imaging was performed after the samples thawed. Because of this process, cryo-TEM images were taken a few days after sample preparation and after freezing and thawing. Details of cryo-TEM sample preparation have been described elsewhere.[33,55]

2.5. ^{1}H NMR. NMR samples were prepared and irradiated in deuterium oxide instead of H_2O. NaOD was used to adjust the pH. Experiments were performed within 3 h after irradiation at ambient temperature with a Bruker DPX 400 MHz NMR spectrometer in the Department of Chemistry at The Ohio State University.

2.6. Drag Reduction and Heat-Transfer Reduction. The percent drag reduction (%DR) is defined as

$$\%\text{DR} = \frac{f_{\text{water}} - f}{f_{\text{water}}} \times 100\% \quad (2)$$

where f is the friction factor defined as

$$f = \frac{\Delta PD}{2\rho LV^2} \quad (3)$$

where ΔP is the pressure drop across the test section of length L, D is the inner diameter of the tube, ρ is the density of the solution, and V is the mean flow velocity.

The percent heat-transfer reduction (%HTR) is defined as

$$\%\text{HTR} = \frac{Nu_{\text{water}} - Nu}{Nu_{\text{water}}} \times 100\% \quad (4)$$

where Nu is the Nusselt number.

The modified Wilson plot method was used to calculate the Nu of the solution.[27] DR and heat-transfer experiments were carried out on a 25-m-long recirculation system with a 10.2 mm inner diameter and a 6 L volumetric capacity. Details of the experiments and the recirculation system have been described elsewhere.[33]

3. RESULTS AND DISCUSSION

Reversible photoisomerization of ACA in the presence of OHAC was investigated using UV−vis spectroscopy and ^{1}H NMR. The resulting shape of micelles in solution was studied by cryo-TEM, and the rheological properties of the solution were examined by rheometry. Finally, the effects of this reversibility on DR and HTR in a large-scale recirculation system were also studied.

3.1. UV−Vis Spectra. To verify the reversible photoisomerization between *trans*-ACA and *cis*-ACA by light irradiation, UV−vis spectra (Figure 1) were obtained for the

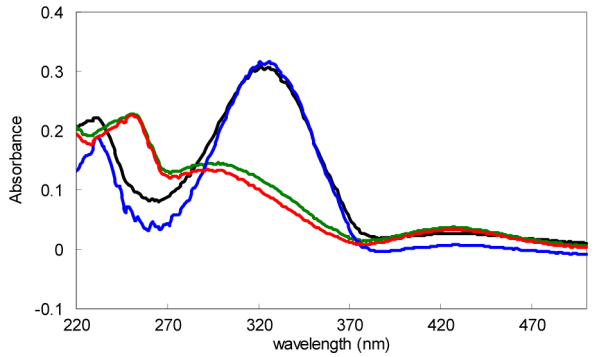

Figure 1. UV−vis spectra of 0.034 mM OHAC + 0.02 mM *trans*-ACA for a fresh sample (black), after UV irradiation (green), after visible light irradiation (blue), and after a second UV irradiation (red).

solution of 0.034 mM OHAC + 0.02 mM ACA after UV and visible light irradiation. In the wavelength range of 220 to 500 nm, all four spectra have three absorbance peaks, denoted as peaks 1−3 from left to right. For the fresh solution containing *trans*-ACA, the three peaks are at 231, 321, and 427 nm, respectively. Among them, peak 2 is a major one and peak 3 was broad and small. After UV irradiation, peaks 1 and 2 shift to 251 and 298 nm, respectively, and peak 3 remains at 427 nm. It should be noted that peak 2 is significantly lower and that peak 3 grows slightly. The changes in spectra correspond to the isomerization of *trans*-ACA to *cis*-ACA.[56,57] The UV-irradiated solution was then irradiated by visible light. The resulting spectrum is essentially the same as the fresh spectrum, indicating that *cis*-ACA reverted to *trans*-ACA. A second UV irradiation following the visible light irradiation again converted the *trans*-ACA spectrum to *cis*-ACA spectrum. These data confirm that the photoisomerization between *trans*-ACA and *cis*-ACA is repeatedly reversible in the presence of OHAC.

3.2. Rheology. DR fluids usually exhibit viscoelastic behavior. The viscoelasticity controls the DR and HTR abilities of these fluids. We probed whether the reversible isomerization

dx.doi.org/10.1021/la304001r | *Langmuir* 2013, 29, 102−109

of ACA would in turn reversibly alter the viscoelasticity of the OHAC/ACA solution. Figure 2a shows the first normal stress

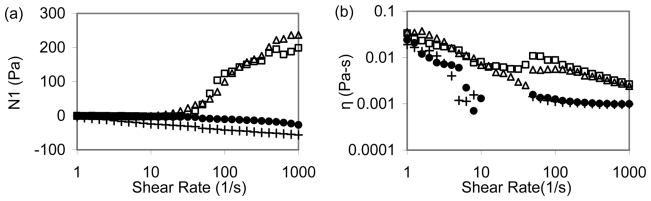

Figure 2. (a) Effects of UV and visible light irradiation on N_1 and (b) the shear viscosity of a 3.4 mM OHAC + 2 mM ACA solution at 25 °C. (□, fresh; ●, UV; Δ, UV followed by visible light; +, UV and visible light followed by UV). The shear viscosity data for solutions after UV irradiation in the shear-rate range of 10 to 50 s^{-1} were negative because of the limited accuracy of the torque sensor.

difference (N_1) versus shear rate at 25 °C for a solution of 3.4 mM OHAC + 2 mM ACA after UV and visible light irradiation. The fresh sample has increasing N_1 against shear rate, which is a typical elastic response. N_1 increases from zero up to ∼240 Pa at 1000 s^{-1}. After UV irradiation, the solution showed waterlike behavior and its N_1 decreased to essentially zero in the shear-rate range of 1 to 1000 s^{-1}. This decrease in N_1 confirms that UV irradiation turns off the viscoelasticity of the solution. After irradiation with visible light, N_1 again increases with shear rate, almost coinciding with that of the fresh solution, indicating that N_1 is restored by visible light irradiation. A second UV irradiation following the visible light irradiation again reduces N_1 to essentially zero in the shear-rate range of 1 to 1000 s^{-1}.

Figure 2b shows the steady-shear viscosity η versus shear rate at 25 °C. Although the fresh solution has shear-thinning behavior over the entire shear-rate range, it also shows modest shear thickening in the shear-rate range of 30 to 50 s^{-1}. This is induced by shear-induced structures (SIS), typical of TLMs.[5,7,8,58,59] UV irradiation reduces the shear viscosity across the entire shear-rate range. In the shear-rate range of 30 to 50 s^{-1}, negative values were measured (not shown). This was because the torque decreased to extremely low values that are below the limit of the rheometer's torque sensor. After visible light irradiation, the shear viscosity was restored to that of the fresh solution. A second UV irradiation reduced the shear viscosity again. All of the data in Figure 2 show that the viscoelasticity of OHAC/ACA solutions can be reversibly tuned by light irradiation at different wavelengths.

3.3. Cryo-TEM. To observe the changes in solution structure directly, cryo-TEM images were taken of fresh samples and samples after UV and visible light irradiation. Figure 3a confirms that TLMs are present in the fresh 3.4 mM OHAC + 2 mM ACA sample. The TLMs are long and extend across the entire image. After UV irradiation, only shorter TLMs and spherical micelles are observed in Figure 3b. Finally, Figure 3c shows that long TLMs have reassembled after visible light irradiation. These observations perfectly correlate with the rheological data (i.e., the presence of TLMs leads to a viscoelastic response whereas the absence leads to a lack of viscoelasticity in the solution).

3.4. ^{1}H NMR. The reversible photoisomerization between *trans*-ACA and *cis*-ACA was also confirmed by ^{1}H NMR analysis. Figure 4a shows the ^{1}H NMR spectra for 2 mM *trans*-ACA before and after irradiation. The fresh sample before irradiation showed large peaks due to *trans*-ACA and small peaks due to *cis*-ACA, with an area ratio of 13.3 (93% trans and 7% cis). After UV irradiation, the *cis*-ACA's peaks grew significantly whereas the *trans*-ACA's peaks diminished. The peak area ratio was 0.11 (10% trans and 90% cis). After visible light irradiation, the *trans*-ACA's peaks increased considerably and the *cis*-ACA's peaks became much smaller. The peak area ratio increased to 2.45 (71% trans and 29% cis). Therefore, ACA reversibly isomerizes between its trans and cis configurations upon UV and visible light irradiation.

Figure 4b shows the ^{1}H NMR spectra for 2 mM *trans*-ACA in the presence of 3.4 mM OHAC before and after irradiation. ACA peaks shifted from those for pure ACA and were also broadened.[52] The fresh sample before irradiation showed large peaks of *trans*-ACA with weak peaks, if any, from *cis*-ACA. The peak-area ratio could not be accurately obtained because of interference from the signal as a result of H_2O (or HOD). After UV irradiation, the *cis*-ACA's peaks grew significantly whereas the *trans*-ACA's peaks diminished. This means that in the presence of surfactant, *trans*-ACA molecules are also converted to *cis*-ACA by UV irradiation. After visible light irradiation, the spectrum looks essentially the same as that of the fresh sample. The *trans*-ACA's peaks increased considerably whereas the *cis*-ACA's peaks became much smaller. This confirms that visible light irradiation converts most *cis*-ACA to *trans*-ACA in the presence of surfactant. In summary, ACA reversibly isomerizes, in the presence of OHAC, between its trans and cis configurations upon UV and visible light irradiation. These

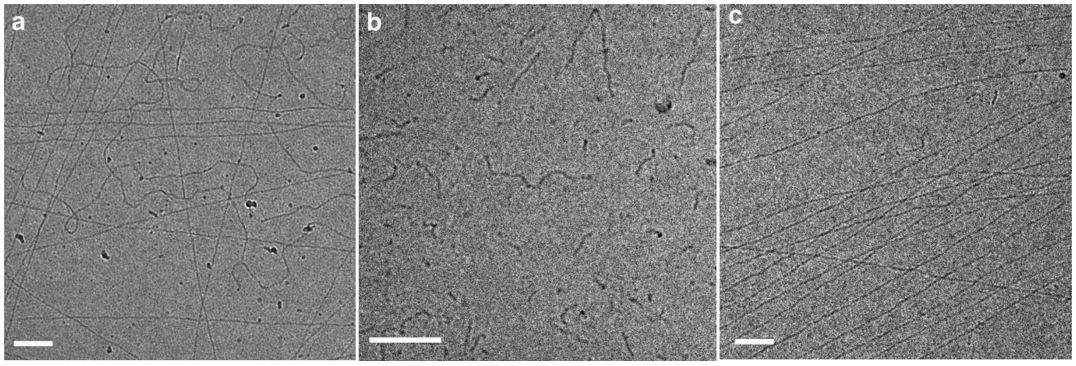

Figure 3. Cryo-TEM images of 3.4 mM OHAC + 2 mM *trans*-ACA sample: (a) fresh sample, image taken 9 days after sample preparation; (b) after UV irradiation, image taken 7 days after sample preparation; and (c) after visible light irradiation, image taken 18 days after sample preparation. Bars correspond to 100 nm.

dx.doi.org/10.1021/la304001r | *Langmuir* 2013, 29, 102−109

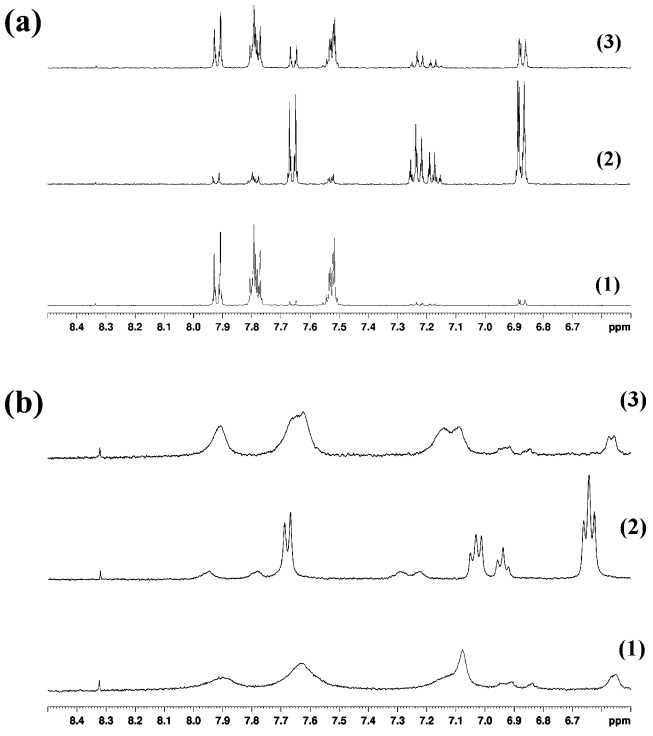

Figure 4. (a) ^{1}H NMR for 2 mM *trans*-ACA (1) before UV irradiation, (2) after UV irradiation, and (3) after UV and visible light irradiation. (b) ^{1}H NMR for 2 mM *trans*-ACA in the presence of 3.4 mM OHCA (1) before UV irradiation, (2) after UV irradiation, and (3) after UV and visible light irradiation.

results are consistent with those reported elsewhere for the mixture of ACA and the EHAC surfactant.[52]

To examine the stability of *trans*-ACA and *cis*-ACA, ^{1}H NMR spectra of aged samples, stored in the light and also in the dark, were obtained at room temperature. In one experiment, a 2 mM ACA solution with a *trans*-ACA to *cis*-ACA ratio of 93:7 did not change when the sample was kept in the dark for 48 h. However, the ratio changed to 70:30 within 24 h in ambient light and remained at this value 48 h after the sample was prepared. In a second experiment, a 2 mM *trans*-ACA solution was irradiated with UV light to give a *trans*-ACA to *cis*-ACA ratio of 15:85. This ratio was maintained for 48 h when the sample was kept in the dark at room temperature, but in ambient light, this ratio changed to 70:30 within 24 h and stayed at this value 48 h after the sample was prepared. Therefore, the ratio of *trans*-ACA to *cis*-ACA for both the fresh and UV-treated ACA solutions converged at 70:30 within 24 h of exposure to ambient light at room temperature.

In the presence of OHAC (3.4 mM), the ACA (2 mM) spectra of both freshly prepared and UV-irradiated samples did not change after at least 24 h in the dark. However, the spectra of the two samples converged to identical spectra within 24 h in ambient light. Thus, ^{1}H NMR results showed that the isomerization between *trans*-ACA and *cis*-ACA was powered by ambient light at room temperature. Therefore, the properties of 3.4 mM OHAC + 2 mM ACA should be stable in closed recirculation systems, where the solution is not subject to any unintended light.

3.5. Drag Reduction and Heat-Transfer Properties. DR data for the 3.4 mM OHAC + 2 mM *trans*-ACA solution at temperatures from 5 to 75 °C are shown in Figure 5. At low *Re*, the solution has a negative %DR, which means that the friction

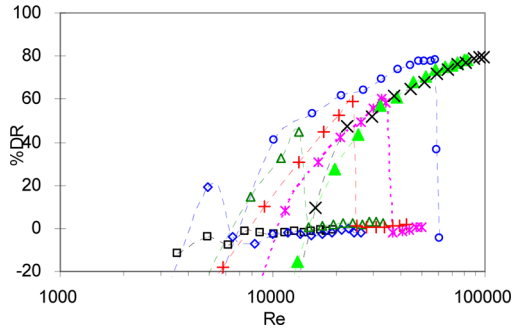

Figure 5. DR vs Reynolds number for an aqueous solution of 3.4 mM OHAC + 2 mM *trans*-ACA at different temperatures (□, 5 °C; blue ◊, 15 °C; green △, 25 °C; red +, 35 °C; pink *, 45 °C; blue ○, 55 °C; green ▲, 65 °C; × , 75 °C).

factor was higher than that of water because of the high shear viscosity of the solution at a low shear rate. Generally, the solution has a better DR ability at higher temperature. At 5 °C, no DR is observed for the entire Reynolds number (*Re*) range. At 15 °C, %DR has a low peak (19%) at a *Re* of 5000. As temperature increases, the solution shows DR over a wider range of *Re*. The DR ranges are 6500−14 800, 7500−25 000, 11 000−36 700, and 7000−60 000 at 25, 35, 45, and 55 °C, respectively. The %DR peak value also grows from 45% at 25 °C to 78% at 55 °C. The *Re* where %DR decrerases rapidly is denoted as the critical *Re*. At this critical *Re*, the shear stress reaches a critical level that destroys TLMs, resulting in more waterlike turbulent behavior in the flow and also the rapid drop in %DR. When the temperature is increased to 65 and 75 °C, %DR reaches 78 and 80%, respectively, at the highest *Re* attainable in our flow system.

Figure 6 shows the DR and heat-transfer properties before and after light irradiation at 25, 35, and 45 °C. The %DR is always lower than %HTR in the DR-effective range of *Re*. They increase together and decrease at the critical *Re*, as reported by others.[18−20] The results demonstrate that UV irradiation turns off both %DR and %HTR in a certain range of *Re* because it shortens the TLMs as shown by cryo-TEM. In our experiments, %DR and %HTR were only partially reduced because the irradiation did not completely convert *trans*-ACA to *cis*-ACA. To destroy the TLMs completely, as observed in the cryo-TEM image (Figure 3b), a higher-powered UV lamp with wavelength narrowed to near 321 nm should be used to irradiate large quantities of solution for a longer period of time.

The range of *Re* in which %DR and %HTR are both reduced is referred to as the responsive range of *Re*. Figure 6 shows that this responsive range of *Re* is widest at 45 °C, indicating that the effect of light irradiation is more pronounced at higher temperatures. This offers a wider responsive range of *Re* to manipulate. Because of the limitations of our apparatus, no heat-transfer experiments were performed above 45 °C, but a wider span is expected at temperatures above 45 °C as the solution is effectively drag-reducing up to 75 °C. Although the critical *Re* of UV-treated solution did not change much as the temperature increased from 25 to 45 °C, the critical *Re* of fresh solution and restored solution increased significantly from ∼13 000 to ∼30 000. This significant increase might be due to the increased flexibility of the TLMs and higher reassembly rates of TLMs at higher temperatures, but for the UV-treated solution, these two factors have little effect on the shorter micelles. Visible light irradiation restored %DR and %HTR to almost the

dx.doi.org/10.1021/la304001r | *Langmuir* 2013, 29, 102−109

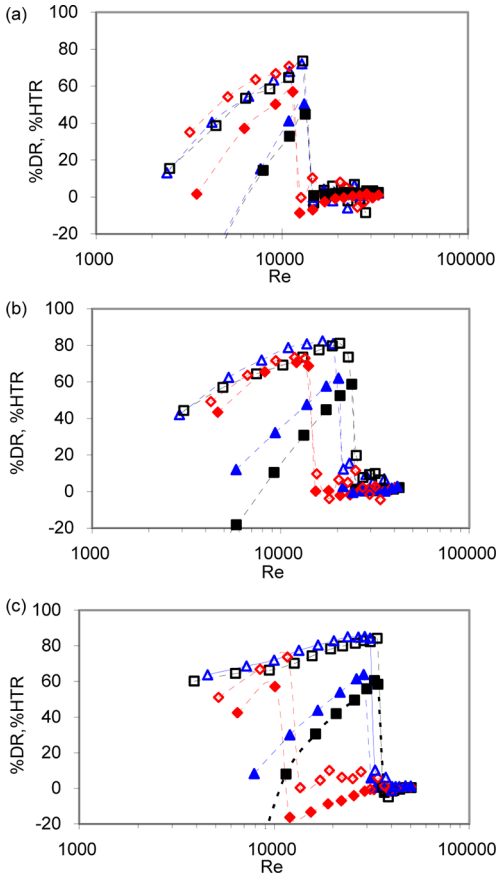

Figure 6. DR and HTR vs Reynolds number for an aqueous solution of 3.4 mM OHAC + 2 mM *trans*-ACA after irradiation at different temperatures. (a) 25, (b), 35, and (c) 45 °C. Legend: □, %HTR of a fresh sample; ■, %DR of a fresh sample; red ◊, %HTR of UV-irradiated sample; red ♦, %DR of UV-irradiated sample; blue △, % HTR of a sample after UV and visible light irradiation; blue ▲, %DR of a sample after UV and visible light irradiation;.

same level. The critical *Re* at each temperature was also restored to approximately the same value as the fresh solution. The small differences in critical *Re* between the fresh solution and the visible-light-irradiated solution were probably caused by the incomplete isomerization of *cis*-ACA to *trans*-ACA. Longer and more intense irradiation should enable a full recovery of the critical *Re*.

In short, DR was suppressed and heat transfer was enhanced for OHAC/ACA solution by UV irradiation and were reversed by visible light irradiation. Thus, this drag-reducing solution could be used in suitably designed district heating and cooling systems both to reduce pumping-energy requirements and to maintain effective heat transfer in the heat exchangers.

4. CONCLUSIONS

In district heating and cooling systems, it is desirable to use a smart fluid whose physical properties, such as the extent of drag reduction and heat-transfer capability, can be controlled by external stimuli. The 3.4 mM OHAC + 2 mM *trans*-ACA solution meets this need. This solution can be tuned to have drag-reducing capability during flow and good heat-transfer capability at the heat exchanger. UV irradiation turns off its DR and simultaneously enhances its heat-transfer capability over a range of *Re*. UV irradiation could be applied at the entrance of a heat exchanger so that the heat exchanger will perform better. Visible light irradiation of the UV-irradiated solution restores its drag-reducing capability and reduces its heat-transfer capability at the same time. This visible light irradiation can be applied to the exit of the heat exchanger so that DR is restored. The reversible changes stem from the reversible photoisomerization between *trans*-ACA and *cis*-ACA, as confirmed by UV−vis and ^{1}H NMR spectra. The ^{1}H NMR spectra also suggested that *trans*-ACA assembles with OHAC to form aggregates. It is possible that *cis*-ACA also forms aggregates with OHAC, but these clearly have different properties than those formed between *trans*-ACA and OHAC. Long TLMs were observed in cryo-TEM images for both the fresh solution and the restored solution. Significantly shortened micelles were found in small quantities after UV irradiation. The changes in micelles were also reflected in reversible changes in rheological properties: shear viscosity and N_1. Thus, this study highlights the potential of switching on the EHT mode of a photoresponsive fluid at the inlet of a heat exchanger and switching on the DR mode at the outlet in a recirculating system. This study also introduces a potential application for other stimuli-responsive smart fluids.

AUTHOR INFORMATION

Corresponding Author

*E-mail: zakin.1@osu.edu.

Notes

The authors declare no competing financial interest.

ACKNOWLEDGMENTS

This work was supported by the National Science Foundation (NSF CBET-0933295) and a Presidential Fellowship from The Ohio State University to H.S. We thank Prof. Robert. S. Brodkey in the Department of Chemical and Biomolecular Engineering at The Ohio State University for providing the UV lamp. The cryo-TEM work was performed at the Technion Laboratory for Electron Microscopy of Soft Matter, supported by the Technion Russell Berrie Nanotechnology Institute (RBNI).

REFERENCES

(1) Porte, G.; Poggi, Y.; Appel, J.; Maret, G. Large micelles in concentrated solutions. The second critical micellar concentration. *J. Phys. Chem.* **1984**, *88*, 5713−5720.

(2) Kumar, S.; Naqvi, A. Z.; Kabir-ud-Din. Micellar morphology in the presence of salts and organic additives. *Langmuir* **2000**, *16*, 5252−5256.

(3) Oelschlaeger, C.; Waton, G.; Candau, S. J. Rheological behavior of locally cylindrical micelles in relation to their overall morphology. *Langmuir* **2003**, *19*, 10495−10500.

(4) Kuperkar, K.; Abezgauz, L.; Danino, D.; Verma, G.; Hassan, P. A.; Aswal, V. K.; Varade, D.; Bahadur, P. Viscoelastic micellar water/CTAB/$NaNO_3$ solutions: rheology, SANS and cryo-TEM analysis. *J. Colloid Interface Sci.* **2008**, *323*, 403−409.

(5) Hu, Y.; Matthys, E. F. Rheological and rheo-optical characterization of shear-induced structure formation in a nonionic drag-reducing surfactant solution. *J. Rheol. (Melville, NY, U.S.)* **1997**, *41*, 151−166.

(6) Ge, W.; Shi, H.; Zakin, J. L. Rheo-optics of cationic surfactant micellar solutions with mixed aromatic counterions. *Rheol. Acta* **2012**, *51*, 249−258.

(7) Lin, Z.; Lu, B.; Zakin, J. L.; Talmon, Y.; Zheng, Y.; Davis, H. T.; Scriven, L. E. Influence of surfactant concentration and counterion to surfactant ratio on rheology of wormlike micelles. *J. Colloid Interface Sci.* **2001**, *239*, 543−554.

(8) Wunderlich, I.; Hoffmann, H.; Rehage, H. Flow birefringence and rheological measurements on shear induced micellar structures. *Rheol. Acta* **1987**, *26*, 532−542.
(9) Zakin, J. L.; Lu, B.; Bewersdorff, H. Surfactant drag reduction. *Rev. Chem. Eng.* **1998**, *14*, 253.
(10) Aly, W. I. A.; Inaba, H.; Haruki, N.; Horibe, A. Drag and heat transfer reduction phenomena of drag-reducing surfactant solutions in straight and helical pipes. *J. Heat Transfer* **2006**, *128*, 800−810.
(11) Ge, W.; Kesselman, E.; Talmon, Y.; Hart, D. J.; Zakin, J. L. Effects of chemical structures of para-halobenzoates on micelle nanostructure, drag reduction and rheological behaviors of dilute CTAC solutions. *J. Non-Newtonian Fluid Mech.* **2008**, *154*, 1−12.
(12) Shi, H.; Wang, Y.; Fang, B.; Huggins, J. T.; Huber, T. R.; Zakin, J. L.Enhancing heat transfer of drag reducing surfactant solution by an HEV static mixer with low pressure drop. *Adv. Mech. Eng.* **2011**, 315943
(13) Gasljevic, K.; Matthys, E. F. On saving pumping power in hydronic thermal distribution systems through the use of drag-reducing additives. *Energy Build.* **1993**, *20*, 45−56.
(14) Yang, J. Viscoelastic wormlike micelles and their applications. *Curr. Opin. Colloid Interface Sci.* **2002**, *7*, 276−281.
(15) Krope, A.; Lipus, L. C. Drag reducing surfactants for district heating. *Appl. Therm. Eng.* **2010**, *30*, 833−838.
(16) Blankinship, S. An old idea is new again. *Power Eng.* **2007**, *111*, 62.
(17) Zhang, Y.; Schmidt, J.; Talmon, Y.; Zakin, J. L. Co-solvent effects on drag reduction, rheological properties and micelle microstructures of cationic surfactants. *J. Colloid Interface Sci.* **2005**, *286*, 696−709.
(18) White, A. Heat transfer characteristics of dilute polymer solutions in fully rough pipe flow. *Nature* **1970**, *227*, 486−487.
(19) Matthys, E. F. Heat transfer, drag reduction, and fluid characterization for turbulent flow of polymer solutions: recent results and research needs. *J. Non-Newtonian Fluid Mech.* **1991**, *38*, 313−342.
(20) Aguilar, G.; Gasljevic, K.; Matthys, E. F. Asymptotes of maximum friction and heat transfer reductions for drag-reducing surfactant solutions. *Int. J. Heat Mass Transfer* **2001**, *44*, 2835−2843.
(21) Paterson, R. W.; Abernathy, F. H. Turbulent flow drag reduction and degradation with dilute polymer solutions. *J. Fluid Mech.* **1970**, *43*, 689−710.
(22) Kim, C. A.; Kim, J. T.; Lee, K.; Choi, H. J.; Jhon, M. S. Mechanical degradation of dilute polymer solutions under turbulent flow. *Polymer* **2000**, *41*, 7611−7615.
(23) Gyr, A.; Bühler, J. Secondary flows in turbulent surfactant solutions at maximum drag reduction. *J. Non-Newtonian Fluid Mech.* **2010**, *165*, 672−675.
(24) Tamano, S.; Itoh, M.; Kato, K.; Yokota, K. Turbulent drag reduction in nonionic surfactant solutions. *Phys. Fluids* **2010**, *22*, 055102−055112.
(25) Kawaguchi, Y.; Segawa, T.; Feng, Z.; Li, P. Experimental study on drag-reducing channel flow with surfactant additives—spatial structure of turbulence investigated by PIV system. *Int. J. Heat Fluid Flow* **2002**, *23*, 700−709.
(26) Li, F.; Kawaguchi, Y.; Yu, B.; Wei, J.; Hishida, K. Experimental study of drag-reduction mechanism for a dilute surfactant solution flow. *Int. J. Heat Mass Transfer* **2008**, *51*, 835−843.
(27) Qi, Y. *Investigation of Relationships among Microstructure, Rheology, Drag Reduction and Heat Transfer of Drag Reducing Surfactant Solutions*. Ph.D. Dissertation, The Ohio State University, Columbus, OH, 2002.
(28) Qi, Y.; Kawaguchi, Y.; Lin, Z.; Ewing, M.; Christensen, R. N.; Zakin, J. L. Enhanced heat transfer of drag reducing surfactant solutions with fluted tube-in-tube heat exchanger. *Int. J. Heat Mass Transfer* **2001**, *44*, 1495−1505.
(29) Li, P.; Kawaguchi, Y.; Daisaka, H.; Yabe, A.; Hishida, K.; Maeda, M. Heat transfer enhancement to the drag-reducing flow of surfactant solution in two-dimensional channel with mesh-screen inserts at the inlet. *J. Heat Transfer* **2001**, *123*, 779−789.
(30) Qi, Y.; Kawaguchi, Y.; Christensen, R. N.; Zakin, J. L. Enhancing heat transfer ability of drag reducing surfactant solutions with static mixers and honeycombs. *Int. J. Heat Mass Transfer* **2003**, *46*, 5161−5173.
(31) Zhou, T.; Leong, K. C.; Yeo, K. H. Experimental study of heat transfer enhancement in a drag-reducing two-dimensional channel flow. *Int. J. Heat Mass Transfer* **2006**, *49*, 1462−1471.
(32) Qi, Y.; Weavers, L. K.; Zakin, J. L. Enhancing heat-transfer ability of drag reducing surfactant solutions with ultrasonic energy. *J. Non-Newtonian Fluid Mech.* **2003**, *116*, 71−93.
(33) Shi, H.; Wang, Y.; Fang, B.; Talmon, Y.; Ge, W.; Raghavan, S. R.; Zakin, J. L. Light-responsive threadlike micelles as drag reducing fluids with enhanced heat-transfer capabilities. *Langmuir* **2011**, *10*, 5806−5813.
(34) Lu, B.; Li, X.; Scriven, L. E.; Davis, H. T.; Talmon, Y.; Zakin, J. L. Effect of chemical structure on viscoelasticity and extensional viscosity of drag-reducing cationic surfactant solutions. *Langmuir* **1998**, *14*, 8−16.
(35) Smith, B. C.; Chou, L. C.; Zakin, J. L. Measurement of the orientational binding of counterions by nuclear magnetic resonance measurements to predict drag reduction in cationic surfactant micelle solutions. *J. Rheol.* **1994**, *38*, 73−83.
(36) Lin, Z.; Zakin, J. L.; Zheng, Y.; Davis, H. T.; Scriven, L. E.; Talmon, Y. Comparison of the effects of dimethyl and dichloro benzoate counterions on drag reduction, rheological behaviors, and microstructures of a cationic surfactant. *J. Rheol.* **2001**, *45*, 963−981.
(37) Wolff, T.; Kerperin, K. J. Influence of solubilized 2,2,2-trifluoro-1-(9-anthryl)-ethanol and its photodimerization on viscoelasticity in dilute aqueous cetyltrimethylammonium bromide solutions. *J. Colloid Interface Sci.* **1993**, *157*, 185−195.
(38) Yu, X.; Wolff, T. Rheological and photorheological effects of 6-alkyl coumarins in aqueous micellar solutions. *Langmuir* **2003**, *19*, 9672−9679.
(39) Lehnberger, C.; Wolff, T. Photorheological effects in aqueous micellar tetramethylammoniumhydrogen-2-dodecyl malonate via photodimerization of acridizinium bromide. *J. Colloid Interface Sci.* **1999**, *213*, 187−192.
(40) Ketner, A. M.; Kumar, R.; Davies, T. S.; Elder, P. W.; Raghavan, S. R. A simple class of photorheological fluids: surfactant solutions with viscosity tunable by light. *J. Am. Chem. Soc.* **2007**, *129*, 1553−1559.
(41) Kumar, R.; Ketner, A. M.; Raghavan, S. R. Nonaqueous photorheological fluids based on light-responsive reverse wormlike micelles. *Langmuir* **2010**, *26*, 5405−5411.
(42) Wang, G.; Tong, X.; Zhao, Y. Preparation of azobenzene-containing amphiphilic diblock copolymers for light-responsive micellar aggregates. *Macromolecules* **2004**, *37*, 8911−8917.
(43) Liu, X.; Jiang, M. Optical switching of self-assembly: Micellization and micelle-hollow-sphere transition of hydrogen-bonded polymers. *Angew. Chem., Int. Ed.* **2006**, *45*, 3846−3850.
(44) Yoshida, E.; Ohta, M. Preparation of micelles with azo dye and UV absorbent at their cores or coronas using non-amphiphilic block copolymers. *Colloid Polym. Sci.* **2007**, *285*, 431−439.
(45) Ruchmann, J.; Fouilloux, S.; Tribet, C. Light-responsive hydrophobic association of surfactants with azobenzene-modified polymers. *Soft Matter* **2008**, *4*, 2098−2108.
(46) Wang, Y.; Zhang, M.; Moers, C.; Chen, S.; Xu, H.; Wang, Z.; Zhang, X.; Li, Z. Block copolymer aggregates with photo-responsive switches: towards a controllable supramolecular container. *Polymer* **2009**, *50*, 4821−4828.
(47) Jochum, F. D.; Theato, P. Thermo- and light responsive micellation of azobenzene containing block copolymers. *Chem. Commun.* **2010**, *46*, 6717−6719.
(48) Chen, C.; Liu, G.; Liu, X.; Li, D.; Ji, J. Construction of photo-responsive micelles from azobenzene-modified hyperbranched polyphosphates and study of their reversible self-assembly and disassembly behaviours. *New J. Chem.* **2012**, *36*, 694−701.

(49) Sakai, H.; Orihara, Y.; Kodashima, H.; Matsumura, A.; Ohkubo, T.; Tsuchiya, K.; Abe, M. Photoinduced reversible change of fluid viscosity. *J. Am. Chem. Soc.* **2005**, *127*, 13454−13455.
(50) Matsumura, A.; Tsuchiya, K.; Torigoe, K.; Sakai, K.; Sakai, H.; Abe, M. Photochemical control of molecular assembly formation in a catanionic surfactant system. *Langmuir* **2011**, *27*, 1610−1617.
(51) Raghavan, S. R.; Ketner, A. M.; Kumar, R. Photorheological Fluids Made Easy: Light-Sensitive Wormlike Micelles Based on Common Inexpensive Surfactants. *The XVth International Congress on Rheology*, Monterey, CA, August 3−8, 2008.
(52) Oh, H.; Ketner, A. M.; Heymann, R.; Kesselman, E.; Danino, D.; Falvey, D.; Raghavan, S. R. Reversible Photorheological Fluids Induced by Transition between Vesicles and Wormlike Micelles in Aqueous System. *243rd ACS National Meeting*, San Diego, CA, March 25−29, 2012.
(53) Anspon, H. D. *p*-Phenylazobenzoic acid. *Org. Synth.* **1945**, *25*, 86−7.
(54) Macosko, C. W. *Rheology: Principles, Measurements, and Applications*; VCH: New York, 1994.
(55) Talmon, Y. In *Seeing Giant Micelles by Cryogenic-Temperature Transmission Electron Microscopy (Cryo-TEM)*; Zana, R., Kaler, E. W., Eds.; Surfactant Science Series 140; CRC Press: New York, 2007; pp 163−178.
(56) Baena, M. J.; Espinet, P.; Folcia, C. L.; Ortega, J.; Etxebarria, J. Photoisomerizable metallomesogens and soft crystals based on orthopalladated complexes. *Inorg. Chem.* **2010**, *49*, 8904−8913.
(57) Sortino, S.; Petralia, S.; Di Bella, S.; Tomasulo, M.; Raymo, F. M. A multistate ensemble of molecular switches. *New J. Chem.* **2006**, *30*, 515−517.
(58) Liu, C.; Pine, D. J. Shear-induced gelation and fracture in micellar solutions. *Phys. Rev. Lett.* **1996**, *77*, 2121−2124.
(59) Oda, R.; Narayanan, J.; Hassan, P. A.; Manohar, C.; Salkar, R. A.; Kern, F.; Candau, S. J. Effect of the lipophilicity of the counterion on the viscoelasticity of micellar solutions of cationic surfactants. *Langmuir* **1998**, *14*, 4364−4372.